Journal of Nuclear Materials 162–164 (1989) 904–909
North-Holland, Amsterdam

MODELING OF PARTICLE–SURFACE REFLECTIONS INCLUDING SURFACE ROUGHNESS CHARACTERIZED BY FRACTAL GEOMETRY

D.N. RUZIC and H.K. CHIU

University of Illinois, Department of Nuclear Engineering, 103 S. Goodwin Avenue, Urbana, IL 61801, USA

Key words: fractal geometry, surface roughness, reflection

The interactions of ions and neutral atoms with surfaces are important for all edge plasma calculations. However, current models treat surfaces as virtually flat two-dimensional objects. To solve this problem in a realistic manner, surface roughness has been added into the TRIM and Embedded Atom Method (EAM) computer codes through the use of fractals. A fractal is a geometric construct with noninteger dimension. Real surfaces have fractal dimensions between 2 and 3 which can be determined experimentally by using the BET gas adsorption method. Inclusion of surface roughness is particularly important at energies below 100 eV and at grazing angles of incidence. Results show that at grazing incidence the particle number and energy reflection coefficients are reduced by a factor of approximately two when even small amounts of surface roughness are included in the models.

1. Introduction

Knowledge about reflection of ions and neutral atoms from surfaces is very important to controlled fusion, plasma processing, and plasma rocket propulsion. In controlled fusion, accurate values of R_n, the number of reflected particles divided by the number of incident particles, and R_e, the total energy of the reflected particles divided by the total energy of the incident particles, are needed to determine hydrogen recycling, impurity redeposition, neutral density calculations, and plasma edge-energy balance. The reflection coefficients are especially needed for incident energies below 100 eV, where experimental data is largely unavailable [1].

There are two computer simulations which are widely used to obtain these values: TRIM [2], which has recently been modified to account for a uniform surface barrier potential extending its use to lower energies [3,4], and the EAM molecular dynamics code [5,6]. Both of these codes treat the surface as being virtually flat with no surface structures. Real surfaces used in fusion devices and other engineering applications are not flat at the microscopic level [7–9]. Especially at low incident particle energies, surface roughness can greatly effect the values of R_e, R_n, and the reflected particle energy distribution.

Previous attempts to model surface roughness have used symmetric ridges [10], or other artificial geometries that could not be connected to observed surface roughness measurements. This work incorporates surface roughness through the statistical use of fractal geometry [11] into the TRIM and the EAM codes. In the molecular-size range, the surfaces of most materials are fractals [12]. Their fractal dimension, D, is measurable through surface adsorption techniques such as the BET method [13]. For example, at the molecular level, the fractal dimension, D, of Vulcan 3G graphite [14] is 2.07 ± 0.01; D of Carbon Black [14] is 2.25 ± 0.09; and D of Activated Alumina [15] is 2.79 ± 0.03. These fractal dimensions may serve only as upper limits if the sample surfaces contain very large scale cracks or pores.

2. Fractal modeling

On a perfectly flat plane, the area of the plane is proportional to the radius of the measuring device used to blanket the surface (an adsorbed gas atom for example) to the 2.00 power. The same area results regardless of the size of the measuring device. On a rough surface, the area of the surface depends on the size of the measuring device. A large sized adsorbate would cover up many fissures that a small size adsorbate could coat. A rough surface is a fractal if it is self-similar at a variety of scales. Therefore, if a plot of the log of the adsorbate radius versus the log of the number of ad-

0022-3115/89/$03.50

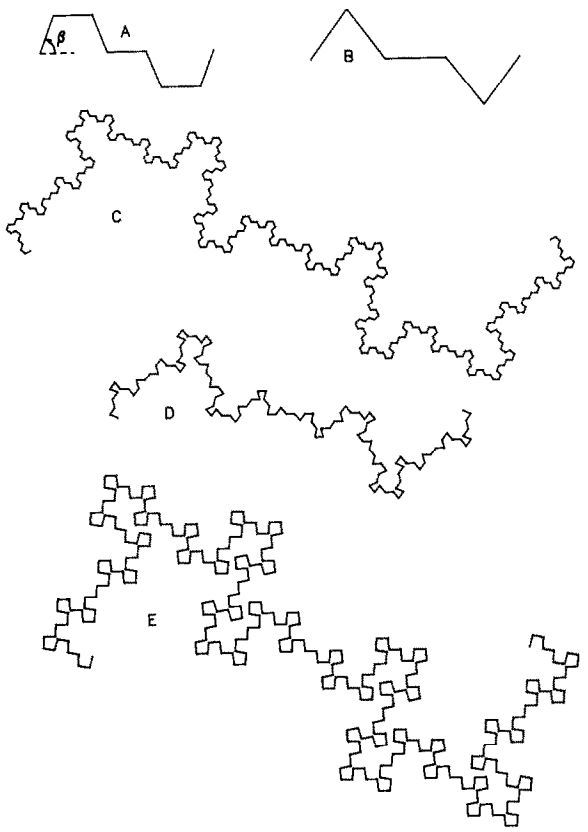

Fig. 1. (a) Generator for fractal intersection surface A. Beta is the generator angle which determines the fractal dimension. (b) Generator for fractal intersection surface B. (c) Fractal intersection surface A with $D = 1.30$. (d) Fractal intersection surface B with $D = 1.30$. (e) Fractal intersection surface A with $D = 1.70$.

sorbate molecules is a straight line, the surface is fractal, and its dimension is related to the slope of that curve. Fractal surfaces have "areas" that are proportional to the radius of the measuring device to the D power. A flat plane has a fractal dimension, D, of exactly 2.00. A fractal surface has a D between 2.00 and 3.00.

The TRIM code is a binary collision model. In it, a scattering plane is defined by the incident particle's trajectory, the location it makes a scattering event, and the particle's new trajectory. This plane makes an intersection with the surface. If the surface was perfectly flat ($D = 2.00$), the intersection would be a straight line with dimension $D = 1.00$. The intersection with a fractal surface is not a line. It is another fractal surface with dimension $D - 1.00$.

Fig. 1 (a and b) shows the fractal generators used to create the intersection surfaces employed in the TRIM code. These generators are volume conserving, have a flat center, and have equal segment lengths. Fig. 1 (c, d and e) show some of the actual intersection surfaces. The length of the individual line segments in a interaction surface was scaled to be approximately 1.7 Å – half the lattice spacing of a Ni fcc unit cell. This dimension was chosen as the minimum extent of the fractal character since it is the shortest perpendicular distance between any two Ni atoms. Variations of less than ± 0.3 Å for this parameter had almost no effect in the simulation. The overall extent of the fractal intersection surface was chosen to be much greater than the mean range of the particle in the solid. This was necessary since merely repeating the same structure adjacent to the original one does not preserve the fractal dimension. The D of these surfaces are related to the angle β by the relations [11]:

$$\text{surface A:} \quad D = \frac{\log 7}{\log(3 + 4\cos\beta)},$$

$$\text{surface B:} \quad D = \frac{\log 5}{\log(1 + 4\cos\beta)}.$$

In this fractal TRIM simulation, the particles start above the center of the fractal surface within a random vertical range. Their initial trajectory is determined by this initial placement and α, the angle with respect to the global surface normal. Then a subroutine is used which determines the particle's intersection point with the surface, and the particle is placed just inside the surface at that location with the same trajectory. TRIM then proceeds as usual: A mean free path is calculated, and an interaction point is determined.

Planar TRIM then determines whether this new interaction point is outside of the flat surface. If it is, and the particle has enough perpendicular energy to penetrate the surface barrier potential, the particle is tallied as a reflection. If the particle does not have enough energy it is placed one mean free path below the surface and its angle of incidence with the surface is specularly reflected. If the interaction point is still inside the surface, TRIM continues. In fractal TRIM a subroutine is used which determines the distance to the surface, DTS, along the new trajectory and the total distance in the fractal, DIF. This is necessary because merely crossing the surface, even with enough perpendicular energy, is no guarantee that the particle will escape. If the mean free path is greater than DIF, the particle may reflect depending on its energy. If the mean free path is greater than DTS but less than DIF, the simulation is *restarted* using the current energy of the particle and an incident angle, α, equal to the angle with respect to the normal of the *second* surface crossed.

Since the intersection surface is only a statistical representation of the intersection of the scattering plane, restarting the particle is equivalent to continuing a fully three dimensional flight history. If the mean free path is less than DTS, the simulation continues.

As in planar TRIM, if the particle does not have enough perpendicular energy to overcome the surface barrier it does not continue along that path. Unlike planar TRIM, a random bounce angle about the specular reflected angle is chosen, and the particle's position is not automatically lowered. In both planar and fractal TRIM the flight stops when the particle's energy is reduce below 1 eV. To monitor the computations of fractal TRIM, the number of interaction steps, restarts and bounces is tabulated for each flight.

The EAM is a molecular dynamic simulation which considers a particle's interaction with all of its neighbors at each time step. The entire lattice is adjusted with the incident particle receiving no special treatment. The immense number of interactions require significant computational resources which limits the number of atoms that can be simulated. However, these interactions must be considered since the collision process is not truly binary. These collective effects must be included to properly conserve energy and are especially important at low energies less than approximately 10 eV.

Fractal geometry was incorporated into the Embedded Atom Method using a different technique [16] than the one used in fractal TRIM. Atoms were added on to a plane surface in a fractal manner and the dynamics of the code were unchanged. Fig. 2 shows a contour map of one of the $D = 2.1$ surface that was used. The smallest fractal cell is the 3 by 3 unit cell structure. On the 9 by 9 drawing, one can see that this simple pyramid has been repeated in a self-similar fashion. In the simulation only the 6 by 6 structure was needed. Excursions through one side were continued by having the particle enter into the opposite side. Though this does not preserve fractal dimension, the number of such adjustments was small. In order to speed computations, new forces were calculated every 30th step for particles far from the incident hydrogen atom. A comparison to calculations done at every step showed no appreciable difference. Initial positions were 15 Å above the highest point on the surface, randomly spaced in x and y. The simulation ended when the particles were once again 15 Å above the highest surface feature, 25 Å below the surface, or slowed to energies less than 1 eV. Even after 600 time steps of 0.001 ps, some flight histories did not meet these criteria. Those that were within 3 Å of the surface, had an outward directed velocity and a final kinetic energy greater than the work function were tallied as reflections. Those which were below 3 Å, had an inward directed velocity and a negative potential energy were tallied as absorptions. Still, some flight histories remained. They were labeled "indeterminate" and not included in the calculation of R_n and R_e.

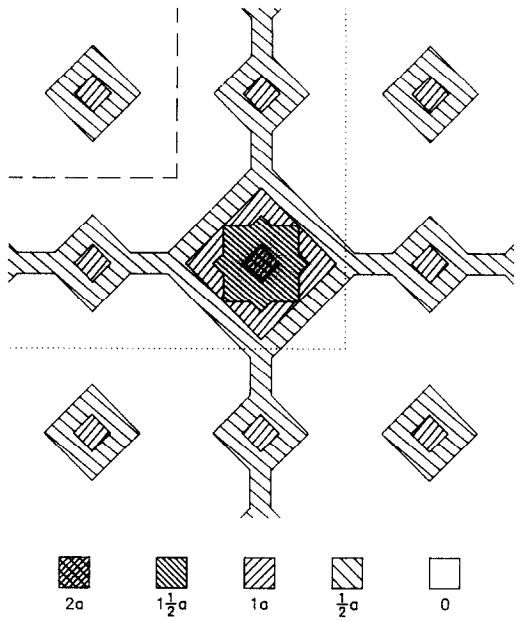

Fig. 2. Contour relief map of the $D = 2.1a$ (hills) surface used with the EAM code. The lattice constant, a, was 3.52 A. The generator for the fractal surface is the 3×3 unit cell area in the upper left corner. The surface wa pieced together by placing adjacent 6×6 unit cell structures next to each other (dotted line).

3. Results

Fractal and planar TRIM were run on a Cray XMP-48. Neither code calculated sputtering, and fractal TRIM has not yet been vectorized. For H incident on Ni at 50 eV with $\alpha = 0$ using fractal surface A with $D = 2.30$, the average flight took 43 ms of CPU time for fractal TRIM and 6 ms for planar TRIM. Table 1 shows individual flight statistics for fractal TRIM flights 8971 through 8977 of 50 eV H normally incident on Ni. Each TRIM run presented was run for 10000 flights giving statistical errors in R and R_e of about 2 to 3%. Representative error bars are shown on all the figures.

Fig. 3 shows R_n and R_e as a function of fractal dimension D for 50 eV H incident on Ni at normal

Table 1
Typical fractal TRIM flight statistics

Steps	Starts	Bounces	Emerging energy (eV)	Emerging angle (deg.)
24	3	2	20.4	66.2
57	1	0	Absorbed	
62	5	2	Absorbed	
3	1	0	45.0	47.1
4	1	1	40.8	63.8
56	1	0	Absorbed	
37	4	0	7.8	59.9

incidence ($\alpha = 0°$) and grazing incidence ($\alpha = 75°$). A steeper grazing angle could have been used, but few ions intersect surfaces at very steep angles due to sheath effects. Even with minor roughness, $D = 2.1$, there is a large decrease in the reflection coefficients at grazing incidence compared with the $D = 2.0$ surface. The $D = 2.0$ results were computed using both planar TRIM and fractal TRIM with $D = 2.01$. Both simulations gave almost identical results. As seen in fig. 3, the reflection coefficients reached a minimum near $D = 2.2$ and then increased as the surface became rougher.

Fig. 4 shows a histogram of the number and energy reflected for three of the normal incident cases from fig.

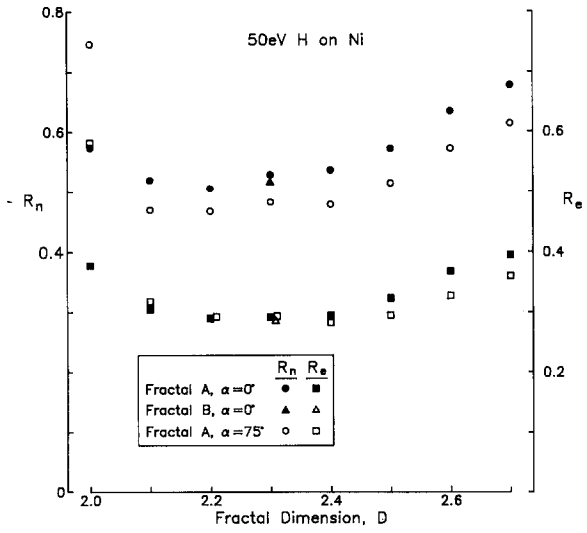

Fig. 3. R_n and R_e versus D for normal incidence ($\alpha = 0°$) and grazing incidence ($\alpha = 75°$) for three different surfaces. H is incident on Ni at 50 eV. The error bars are the size of the data points. Note the large drop-off of R at grazing incidence when D is greater than 2.00.

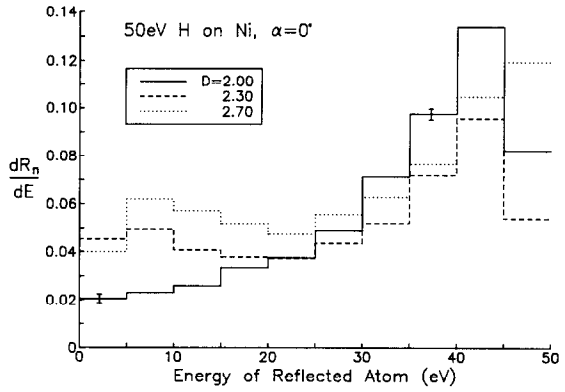

Fig. 4. Histogram of the number of H reflected from a Ni surface at 50 eV. The angle of incidence was normal to the $D = 2.00$, $D = 2.30$, and $D = 2.70$ fractal A surfaces. Note the increase in full energy reflections when $D = 2.70$. Representative error bars are shown.

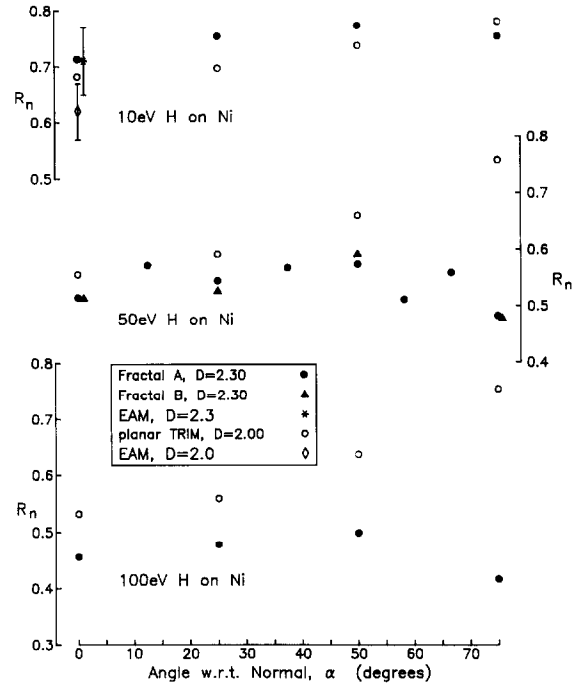

Fig. 5. R_n versus angle of incidence with respect to the surface normal for 10, 50 and 100 eV H on Ni for: fractal surface A, $D = 2.30$; fractal surface B, $D = 2.30$; and planar surface, $D = 2.00$. EAM results for $D = 2.0$ and $D = 2.3$ at 10 eV are also shown. Error bars for TRIM results are the size of the data points. At large angles the planar and fractal results differ by almost a factor of two.

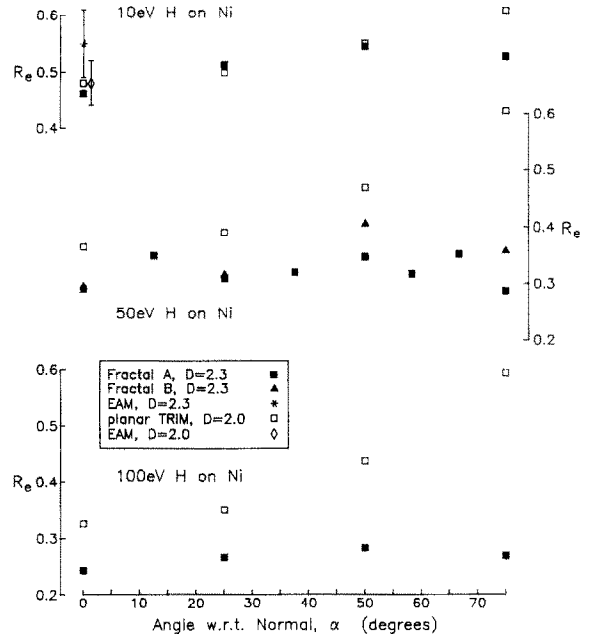

Fig. 6. R_e versus angle of incidence with respect to the surface normal for 10, 50 and 100 eV H on Ni for: fractal surface A, $D = 2.30$; fractal surface B, $D = 2.30$; and planar surface, $D = 2.00$. EAM results for $D = 2.0$ and $D = 2.3$ at 10 eV are also shown. Error bars for TRIM results are the size of the data points. At large angles the planar and fractal results differ by almost a factor of two.

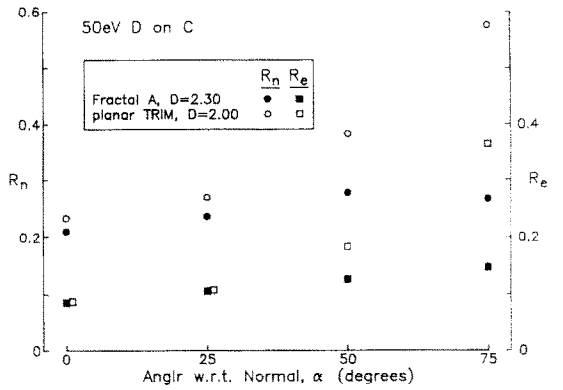

Fig. 7. R_n and R_e versus angle of incidence with respect to the surface normal for 50 eV Deuterium on C for: fractal surface A, $D = 2.30$; and planar surface, $D = 2.00$. Error bars are the size of the data points. At large angles the planar and fractal results differ by more than a factor of two.

3: $D = 2.0$, $D = 2.3$, and $D = 2.7$. The initial decrease in R from $D = 2.0$ to $D = 2.3$ results from more particles being reflected with lower energies, but fewer overall. When D reaches 2.7 there is a large increase in the number of full energy reflections. These are particles which "rattle around in the surface structure" and never reach the bulk where significant energy loss would proceed more quickly. There are 3 to 4 times as many re-starts and bounces than the $D = 2.3$ case and a higher percentage of them can escape. At grazing incidence the effect is similar, but there are even more restarts leading to slightly lower reflection coefficients.

The angular distribution of the reflected particles for all fractal cases is broad and flat with a peak around 45° and virtually no emission near 0° or 90°. As D increases to 2.2, mirror-like reflection of grazing incidence particles is no longer seen.

To confirm the hypothesis that surface roughness can be simulated by fractal dimension, fractal surface B, shown in fig. 1 (b and d), was also used in fractal TRIM. The results for 50 eV H on Ni with $D = 2.3$ are shown in fig. 3, 5 and 6 as triangles. The results match well with surface A even though the surfaces themselves differ.

Figs. 5 and 6 show R_n and R_e as a function of incident angle for 10 eV, 50 eV, and 100 eV, H on Ni for planar TRIM (open symbols) and fractal trim with $D = 2.3$ (filled symbols). Reflection coefficients from rough surfaces do not increase as the incident angle is increased as they do from flat surfaces. In fact, at these energies, the incident angle with respect to the global surface normal makes little difference. Fig. 7 shows R_n and R_e as a function of incident angle for 50 eV

Table 2
fractal EAM flight summary

Surface	Absorb-tions	Reflec-tions	Indeter-minate	R_n	R_e
2.0	83	138	36	0.62 ± 0.05	0.48 ± 0.04
2.1a	81	139	30	0.63 ± 0.05	0.46 ± 0.04
2.1b	63	132	54	0.68 ± 0.06	0.56 ± 0.06
2.3	58	142	44	0.71 ± 0.06	0.55 ± 0.06

deuterium on C. Again, planar TRIM is denoted by open symbols and fractal TRIM with the $D = 2.3$ surface A is denoted by filled symbols. A similar independence of incident angle is seen for the rough surface.

The fractal EAM simulation was run on an IBM 3090. Four different surfaces were used with fractal dimensions: 2.0, 2.1, 2.1 and 2.3 A contour map of surfaces "2.1*a*" is shown in fig. 2. The surface "2.1*b*" was significantly different having ridges and furrows instead of hills. In all cases a 10 eV H atom was normally incident on a Ni (100) base lattice. Each flight was broken into time steps of 0.001 ps to ensure energy conservation. The average flight took 6 cpu seconds per step. On the Cray XMP-48 this was reduced to 3 cpu seconds per step, however, tens of cpu minutes were still required per flight. Accordingly, only approximately 250 flights were run for each surface. The breakdown of the histories are shown in table 2.

The R_n and R_e for surfaces 2.0 and 2.3 are shown in figs. 5 and 6 along with the 10 eV results of TRIM. Statistically, the results overlap.

4. Discussion

Surface roughness has a significant effect on the calculation of reflection coefficients at large angles of incidence. Even apparently flat plasma-smoothed surfaces have significant microscopic roughness [8] which could lower R_n and R_e appreciably. Since future fusion devices may have divertor plates or limiters intersecting magnetic field lines at grazing angles, surface roughness should be accounted for in the recycling, energy loss, and neutral density calculations. The algorithm presented here allows such a calculation based upon a measurable parameter of the surface in question.

From these results, reflection coefficients seem to be a function of fractal dimension independent of the fractal generator that was chosen. However, a further refinement in determining the character of the surface roughness is possible using the fractal concept of lacunarity [17]. Two surfaces with the same fractal dimension could have a different gap size. The gap size could be determined by electron micrographs so that further structure to the intersection surface could be added. Additional work under way here also includes the calculation of sputtering coefficients from rough surfaces and experimental measurements of low energy ion reflection [18].

Acknowledgements

We wish to thank and acknowledge the Max-Planck-Institut für Plasmaphysik for permission to use the TRIM code, Sandia National Laboratories at Livermore for permission to use the EAM code, the Educational Development Program of IBM Corporation for support and the use of their IBM 3090, the National Center for Super Computing Applications at the University of Illinois for the use of their Cray XMP-48, and the Presidential Young Investigators Program of the NSF (CBT-84-51599).

References

[1] W. Eckstein and H. Verbeek, Data Compendium for Plasma–Surface Interactions, Chap. 2, Nucl. Fusion, special issue (1984).
[2] J.P. Biersack and L.G. Haggmark, Nucl. Instr. and Meth. 174 (1980) 257.
[3] W. Eckstein and D.B. Heifetz, J. Nucl. Mater. 145–147 (1987) 332.
[4] R. Aratari, W. Eckstein, in: these Proc. (PSI-8), J. Nucl. Mater. 162–164 (1989) 910.
[5] M.S. Daw and M.I. Baskes, Phys. Rev. B29 (1984) 6443.
[6] M.I. Baskes, J. Nucl. Mater. 128 & 129 (1984) 676.
[7] E. Franconi and C. Ferro, J. Nucl. Mater. 128 & 129 (1984) 929.
[8] A.E. Pontau, W.R. Wampler, B.e. Mills, B.L. Doyle, A.F. Wright, M.A. Ulrickson, P.H. LaMarche, H.F. Dylla and S. Fukuda, J. Vac. Sci. Technol. A4 (1986) 1193.
[9] A.E. Pontau, R.A. Causey and J. Bohdansky, J. Nucl. Mater. 145–47 (1987) 775.
[10] N.N. Koborov, V.A. Kurnaev and V.M. Sotnikov, J. Nucl. Mater. 128 & 129 (1984) 691.
[11] B.B. Mandelbrot, The Fractal Geometry of Nature (Freeman, San Fransisco, 1982).
[12] D. Avnir, D. Farin and P. Pfeifer, Nature 308 (1984) 261.
[13] S. Brunaner, P.H. Emmett and E. Teller, J. Am. Chem. Soc. 60 (1938) 309.
[14] D. Avnir, D. Farin and P. Pfeifer, J. Chem. Phys. 79 (1983) 3566.
[15] H. Burns, Jr., D.K. Carpenter, Macromolecules 1 (1968) 384.
[16] H.K. Chiu, The Reflection of Hydrogen off Nickel Surfaces as a Function of Fractal Dimension, MS Dissertation, University of Illinois (1988).
[17] B.B. Mandelbrot, The Fractal Geometry of Nature, Chap. 34 (Freeman, San Fransisco, 1982).
[18] D.N. Ruzic, B.L. Cain, H.K. Chiu, Bult. APS 31 (1986) 1624.